Magnetoresistance oscillations induced by periodically arranged micromagnets (invited)

P. D. Ye, D. Weiss,[a] and R. R. Gerhardts
Max-Planck-Institut für Festkörperforschung, D-70569 Stuttgart, Germany

H. Nickel
Forschungsinstitut der Deutschen Bundespost, D-64295 Darmstadt, Germany

Probing magnetic fields can be done, e.g., by employing the well established Hall effect. Alternatively, we make use of the *ballistic* motion of electrons in high mobility two-dimensional electron systems (2DES) to probe electrically the stray field of periodically arranged micomagnets. We investigate the magnetoresistance of the 2DES underneath arrays of magnetic strips and magnetic dots having periods between 500 nm and 1 μm. The periodic stray field gives rise to pronounced oscillations of the resistivity as a function of a homogeneous (weak) magnetic field. The magnetization orientation of the dots and strips can be aligned in different directions with respect to the current flow through the device. The observed magnetoresistance depends characteristically on the magnetization direction and can be understood in terms of the stray field pattern probed by the electrons. © *1997 American Institute of Physics.* [S0021-8979(97)62508-6]

I. INTRODUCTION

Nanometer scale ferromagnetic particles are expected to display unusual magnetic behavior.[1] Depending on the size of the particles the magnetic properties can be tuned from single domain to multidomain behavior. Arrays of such magnetic ''quantum dots'' may also be of interest for magnetic storage applications where storage densities of 100 Gbit/sq. in. can be envisaged using advanced lithographic techniques. Different routes can be taken to fabricate magnetic structures ranging from the micron to the nanometer regime by using, e.g., electron beam lithography,[2] metalorganic chemical vapor deposition with a tunneling microscope tip[3] or the deposition of sub-monolayer magnetic films on Au(111) surfaces.[4] To investigate the magnetic properties of such small particles large arrays ($\sim 10^6$ in Ref. 2) can be used and the macroscopic stray fields can be measured conventionally. Other methods to obtain magnetic information about individual ultrafine particles involve an elaborate microsusceptometer technique based on dc superconducting quantum interference devices,[5] scanning magnetometers,[6] Hall effect measurements employing two-dimensional electron systems,[7] magnetic force,[8–10] and Lorentz microscopy.[11]

Below we show that the *ballistic motion* of electrons in a two-dimensional electron gas (2DEG) can be used to obtain information about the stray fields of periodically arranged micromagnets deposited on top of semiconductor heterojunctions as is shown in Fig. 1. We find pronounced oscillations of the resistance of the 2DEG as a function of the externally applied magnetic field B_0 reflecting the presence of a periodically modulated magnetic field in the plane of the electron gas (accompanied by a weak electrostatic periodic potential; see below).

II. COMMENSURABILITY EFFECTS IN MODULATED TWO-DIMENSIONAL ELECTRON SYSTEMS

Two-dimensional electron systems can be found in field effect transistor structures or in GaAs-AlGaAs heterojunctions.[12] In GaAs–AlGaAs heterojunctions, e.g., the electrons are trapped in a potential well at the interface between the two materials and carrier motion in growth direction is prohibited while possible along the interface. 2DEG's are known for their peculiar transport properties. In strong magnetic fields, Shubnikov–de Haas oscillations appear in the longitudinal resistivity ρ_{xx}, while the Hall resistance displays quantized values, the quantum Hall or von Klitzing effect.[13,14] These effects are closely connected to the discrete Landau level energy spectrum of the electrons in a magnetic field. At zero or low magnetic fields (and low temperatures) the electrons can travel ballistically over several microns. Effects like electron focusing,[12,15] quantized point

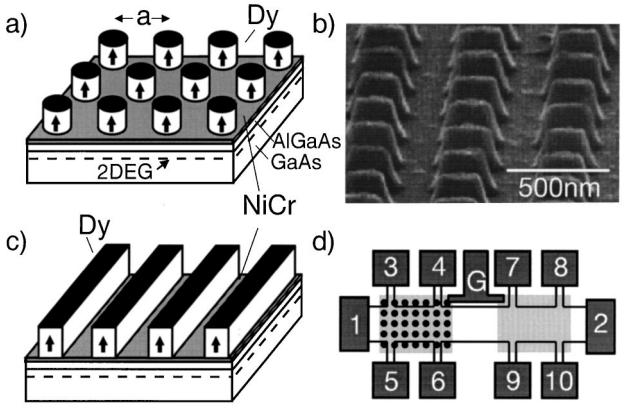

FIG. 1. (a) Sketch of a two-dimensional ferromagnetic Dy dot lattice on top of a GaAs–AlGaAs heterojunction. The corresponding electron micrograph of a tilted sample is shown in (b). Period of the square array: 500 nm, height of the dots 200 nm. (c) Sketch of a one-dimensional ferromagnetic strip lattice. (d) Device geometry containing a dot array and a NiCr coated, unpatterend reference area. The ohmic contacts are numbered while the gate electrode is labeled by G.

[a]Also with: Experimentelle und Angewandte Physik, Universitat Regensburg, D-93040 Regensburg, Germany.

 0021-8979/97/81(8)/5444/5/$10.00

contact resistances,[16,17] or commensurability effects (in lateral superlattices)[18,19] can be found in such systems.

The effect of a weak periodic magnetic field on a two-dimensional electron gas has been predicted to result in an oscillatory magnetoresistance, which reflects the commensurability between the period a of the magnetic field modulation and the classical cyclotron diameter $2R_c$ of the electrons at the Fermi energy E_F.[20–23] For a weak one-dimensional magnetic modulation with modulation amplitude $|B_m|$ much smaller than the external magnetic field $|B_0|$, the magnetoresistance ρ_{xx} oscillates with minima appearing at magnetic fields given by[20–24]

$$2R_c=\frac{2\hbar k_F}{e|B_0|}=\left(\lambda+\frac{1}{4}\right)a, \tag{1}$$

where $\lambda=1,2$ is an integer oscillation index, $k_F=\sqrt{2\pi n_s}$ is the Fermi wavenumber, n_s is the carrier density of the 2DEG, and a is the period of the modulation in x direction. This effect, observed recently,[25–27] is intimately related to the commensurability (Weiss-) oscillations observed in the resistivity ρ_{xx} of a 2DEG with weak electrostatic modulation.[18,28,29] Similar to the electric case, the magnetic modulation modifies the energy spectrum.[20–24]

The degenerate Landau levels are transformed into bands of finite width. The dispersion of these Landau bands provides an additional contribution to the resistivity ρ_{xx}, that only vanishes when the bandwidth becomes zero (flatband condition).[24,28,29] In contrast to Eq. (1), describing the flatband condition for magnetic modulation, the flatband condition for weak electrical modulation reads $2R_c=(\lambda-1/4)a$ with $\lambda=1,2,...$. Hence, ρ_{xx} of a 2DEG with a weak electric modulation displays minima at B_0 fields where in a weak magnetic modulation of the same period a maxima would appear.

To understand the experiments below it is, however, sufficient to consider the *classical* motion of electrons in periodic electrostatic and/or periodic magnetic fields. For the case of a pure electric modulation, the additional contribution to ρ_{xx} has been related to the classical guiding center drift of the cyclotron orbits, which vanishes if the flatband condition holds.[30] This classical picture can be extended to include, in addition to an arbitrary periodic modulation $V_m(\mathbf{r})=\Sigma_{\mathbf{q}\neq 0}V_{\mathbf{q}}e^{i\mathbf{qr}}$ of the electrostatic potential energy of an electron, a weak modulation $B_m(\mathbf{r})=\Sigma_{\mathbf{q}\neq 0}B_{\mathbf{q}}e^{i\mathbf{qr}}$ of the z component of the magnetic field [$\mathbf{q}=(Kn_x,Kn_y)$ with $K=2\pi/a$ and integers n_x, n_y, not simultaneously zero]. Averaging the modulation induced drift of the guiding centers over the unperturbed cyclotron orbits at field B_0,[24,30] we obtain a change in the resistivity

$$\frac{\Delta\rho_{xx}}{\rho_0}=\frac{l_e^2}{2E_F^2}\sum_{\mathbf{q}\neq 0}q_x^2|S|^2, \tag{2}$$

$$S\approx\left(\frac{2}{\pi qR_c}\right)^{1/2}\left[\sigma V_{\mathbf{q}}\cos\left(qR_c-\frac{\pi}{4}\right)+\frac{k_F}{q}\hbar\omega_{\mathbf{q}}\sin\left(qR_c-\frac{\pi}{4}\right)\right], \tag{3}$$

where $\rho_0=1/en_s\mu$ is the zero-field resistivity of the unmodulated 2DEG with the electron mobility μ, $\omega_{\mathbf{q}}=eB_{\mathbf{q}}/m^*$ (m^* is the effective electron mass of GaAs and σ either $+1$ or -1 depending on the direction of the externally applied magnetic field B_0. For a one dimensional (1D) modulation [$\mathbf{q}=(Kn_x,0)$], we find $\Delta\rho_{xy}=\Delta\rho_{yx}=\Delta\rho_{yy}=0$ to leading order in the small parameter $(\mu B)^{-1}$. Equation (2) directly relates the observable resistivity changes to the periodic magnetic field ''landscape.''

III. FABRICATION AND EXPERIMENT

Our samples were prepared from high-mobility GaAs–AlGaAs heterojunctions. The 2DEG was located approximately 100 nm underneath the sample surface. The carrier density n_s and electron mobility μ at 4.2 K were typically $\sim 2.2\times 10^{11}$ cm^{-1} and 1.3×10^6 cm^2/V s in the dark, corresponding to an elastic mean free path of ~ 10 μm, much longer than the spacing of the micromagnets. 50-μm-wide Hall bars, sketched in Fig. 3(d) were fabricated by standard photolithographic techniques. Alloyed AuGe/Ni pads contact the 2DEG. A 10 nm thin NiCr film, evaporated on top of the devices, defines an equipotential plane to avoid electric modulation of the 2DEG. However, strain due to different thermal expansion coefficients of the ferromagnetic grating and the heterojunction always results in a weak electric periodic potential as the sample is cooled down to cryogenic temperatures.[31] The strain-induced electrostatic potential modulation, based on calculations of Davies and Larkin,[32] is shown in Figs. 2(a) and 2(b). The Dy arrays with periods of 500 nm and 1 μm were defined by electron beam lithography on top of the NiCr gates. After developing the exposed PMMA resist, a 200 nm Dy film was evaporated. After lift-off in acetone, ferromagnetic microstructures, like the ones shown in Fig. 1(b), were obtained. Four-point resistance measurements were performed in a ^{4}He cryostat with superconducting coils using standard ac lock-in techniques. A current bias I is applied between contacts 1 and 2 [see Fig. 1(d)] and the measured voltage drop U between, e.g., contact 3 and 4 (7 and 8) and 3 and 5 (7 and 9) give the longitudinal resistivity $\rho_{xx}=wU_x/Il$ and the Hall resistance $\rho_{xy}=U_y/I$ in the patterned (unpatterned) segments of the Hall bar geometry. Here, l/w is the ratio between potential probe separation and width of the Hall bar.

IV. ONE-DIMENSIONAL PERIODIC MAGNETIC FIELDS

Figure 2(c) displays the magnetoresistance of a 2DEG measured for different directions of the magnetization $\mathbf{M}$ in the Dy strips. The direction of $\mathbf{M}$ [see inset of Fig. 2(c)] was adjusted by tilting the sample with respect to the direction of the external magnetic field which, in this case, was swept up to a maximum field of 10 T and then back to $B_0=0$ T. For the resistance measurements the samples were rotated back to such an orientation that the external magnetic field B_0 was applied normal to the plane of the 2DEG (z direction). Because the Dy microstructures used here show pronounced hard magnetic behavior,[26] the imposed magnetization is only slightly changed in the low field region. If the strips are magnetized along their axis essentially no magnetic modula-

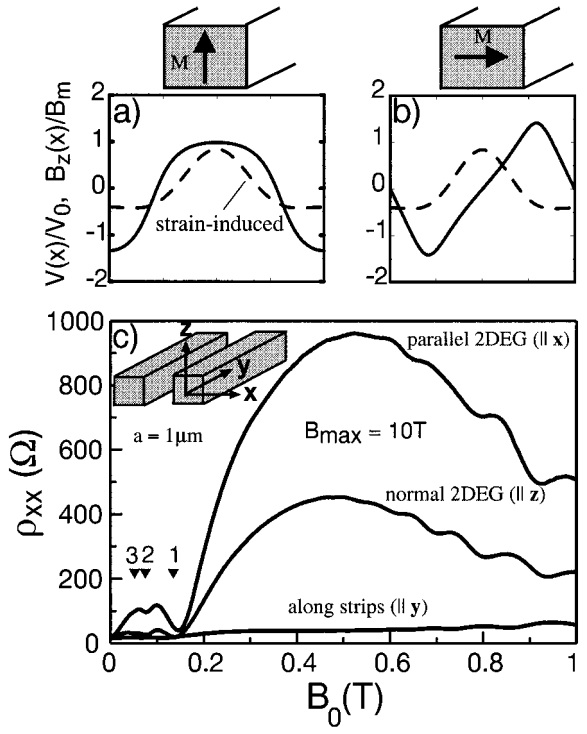

FIG. 2. (a) Periodic magnetic field (z component) and strain induced (dashed) electrostatic periodic potential underneath a metallic strip. (b) As (a) but with a magnetization orientation of the strips parallel to (x direction) the two-dimensional electron gas. Note the phase shift between periodic potential and periodic magnetic field for this magnetization orientation. (c) Resistance of a 2DEG as a function of the externally applied magnetic field B_0 (always pointing in z direction) measured at 4.2 K. Different traces correspond to different directions of the magnetization **M** (see inset). The different amplitudes of the oscillations for $\mathbf{M}\|x$ and $\mathbf{M}\|z$ indicate different strengths of the stray field in the z direction and is probably a consequence of the rectangular shape of the wires.

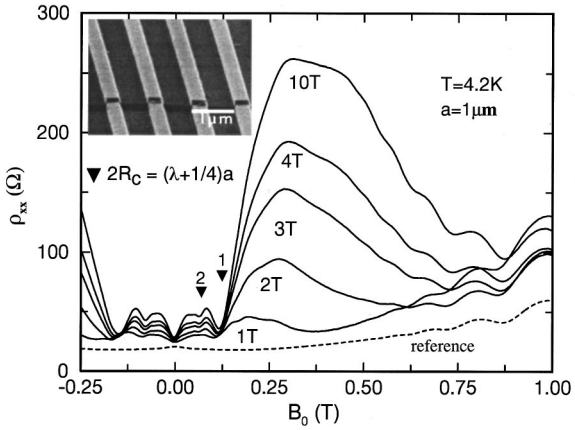

FIG. 3. ρ_{xx} vs external magnetic field B_0 for different $B^{\max}$ sweeps. Filled triangles with positions defined by Eq. (1) mark the flatband condition in a periodic magnetic field. The dashed line is taken from the segment without micromagnets and displays no extra structure. The inset shows an electron micrograph of the Dy strip lattice with period $a=1$ μm.

tion is imposed on the 2DEG, as expected, and the ρ_{xx} trace is virtually independent (on this scale) of the applied magnetic field. The situation changes dramatically if the strips are magnetized either in z or in x direction. The corresponding stray field in the plane of the 2DEG is shown schematically in Figs. 2(a) and 2(b), respectively. In Figs. 2(a) and 2(b) the slope of the conduction band underneath a ferromagnetic strip in GaAs is also shown. The modulation of the electrostatic potential is due to the strain imposed by the metallic microstructures on top of the heterojunction. Pronounced oscillatory behavior dominates ρ_{xx} in Fig. 2(c) with minima at magnetic field positions predicted for *pure* magnetic modulation. Hence, these traces display the *magnetic commensurability oscillations* anticipated by theory. Since on the other hand we know that a strain induced electric modulation is present, we conclude that for the maximum ''conditioning'' field of $B^{\max}=10$ T the strength of our micromagnets covers up the effect of the electrostatic potential modulation.

In Fig. 3 we display the resistivity ρ_{xx} for different strength of the magnetic field $B^{\max}$ applied in the z direction [perpendicular to 2DEG, see Fig. 2(a)]. The traces labeled 1 T–10 T are obtained as follows. After the initial cooldown we first sweep to 1 T and measure the ρ_{xx} trace labeled 1 T from 1 to -0.25 T. Then we sweep to $B^{\max}=2$ T and take the next ρ_{xx} trace in the same B_0 interval. By successively sweeping to higher $B^{\max}$ (again up to 10 T) the magnetic polarization J in the Dy stripes and hence the strength of the resulting periodic field $B_m(x)$ is increased. This enhanced strength affects the magnetoresistance traces. ρ_{xx} displays oscillations with a dramatically growing maximum between $B_0=0.15$ and 0.75 T (the superimposed oscillations above 0.5 T are Shubnikov–de Haas oscillations) For positive B_0, the minima in ρ_{xx} appear at B_0 values expected from Eq. (1) for *magnetic* modulation. A low field magnification (Fig. 4) of the data shown in Fig. 3 illustrates the competition between electric and magnetic modulation. By increasing the magnetization **M** in the strips gradually, starting from $\mathbf{M}\approx 0$, the influence of both the electrostatic periodic potential and the magnetic modulation can clearly be seen.[26] In Fig. 4 the strain-induced electrostatic periodic potential is *in phase* with the periodic magnetic field [maxima of the periodic

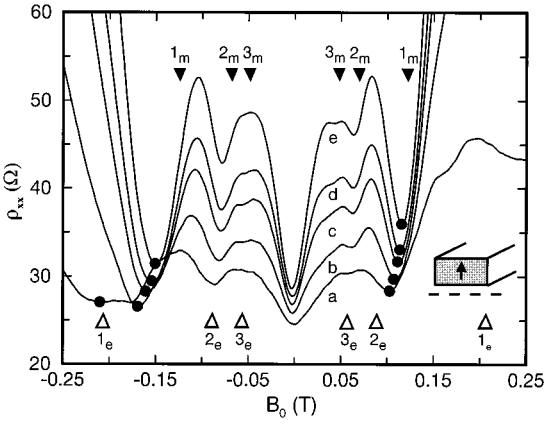

FIG. 4. Low-field magnification of Fig. 3 showing the shift of the ρ_{xx} minima with increasing $B^{\max}$ (from $a=1$ T to $e=10$ T). Full triangles mark the position of the *magnetic* flatband condition (subscript m) while the open triangles mark the *electric* ones (subscript e). The circles highlight the positions of the ρ_{xx} minima used to evaluate the stray field amplitude from the zeros of Eq. (2) (see Ref. 26).

potential and the periodic magnetic field are both underneath the centers of the magnetic strips; see Fig. 2(a)]. In Fig. 4 traces labeled (a)–(e) are also taken for different maximum ''conditioning'' fields $B^{\max}$ between 1 T (a) and 10 T (e). With increasing $B^{\max}$ a richer oscillatory structure unfolds in ρ_{xx} indicating a growing amplitude of the magnetic field modulation. Open triangles mark the expected positions of the minima (flatband condition) for pure electric modulation at $2R_c=(\lambda-1/4)a$ while filled ones mark pure magnetic modulation at $2R_c=(\lambda+1/4)a$. With increasing strength of the magnets [corresponding to growing $B_{\mathbf{q}}$ in Eq. (3)] the minima positions shift from electric-modulation-dominated minima to magnetic-modulation-dominated minima (from 2_e to 1_m for $B_0>0$ and from 1_e to 1_m for $B_0<0$). The asymmetry of the traces with respect to $B_0=0$ is a consequence of changing the sign of σ in Eq. (3).[26] The shift of the minima in Fig. 4 corresponds to a growing magnetic contribution $s_m\equiv(k_F/q)\hbar\omega_{\mathbf{q}}\sin[qR_c-(\pi/4)]$ in Eq. (3), whereas the strain induced contribution, $s_e\equiv V_{\mathbf{q}}\cos[qR_c-(\pi/4)]$, is unaltered. The minima position in ρ_{xx} is determined by the zeros of $|s_m+s_e|^2$. Hence, the shift can be used to estimate the amplitude of the magnetic stray field: assuming a simple sinusoidal modulation $[\mathbf{q}=(2\pi/a,0)]$ we obtain a remanent peak-to-peak modulation of 40 mT for trace (e) at $B_0=0$.[26]

The ''interference'' of electric and magnetic modulation changes drastically if **M** is tilted in the x direction.[24] Now the magnetic modulation suffers a phase shift of $\pi/2$ with respect to the electric one [see Fig. 2(b)]. Such a phase shift, already addressed in Ref. 21 has consequences. While a magnetization in the z direction leads to real Fourier coefficients, that is to a pure cosine expansion of the modulation magnetic field, the magnetization in the x direction leads to purely imaginary coefficients, i.e., a sine expansion. As a result, the Lándau bands no longer become flat since now magnetic and electric modulation are simply added, $|s_m|^2+|s_e|^2$. This additive behavior can clearly be seen in the traces of Fig. 5 where the strips are magnetized parallel to the 2DEG. The dashed trace is taken directly after cooling down the device and the oscillations in ρ_{xx} are perfectly described by a pure electrostatic periodic potential, strain-imposed upon the 2DEG. With increasing $B^{\max}$ the effect of the magnetic field modulation takes over as can be seen from the minima position at the magnetic flatband condition (full triangles). At the magnetic flatband condition $\lambda=1$ near $B_0\sim0.28$ T it is obvious that the ρ_{xx} minimum ''sits'' upon the maximum originating from the electric modulation.

V. TWO-DIMENSIONAL PERIODIC MAGNETIC FIELDS

Figure 6 displays data measured in a two-dimensional periodic magnetic field generated by an array of nanoscale magnetic posts. The size of the arrays investigated was $\sim100\times100\ \mu\text{m}^2$ containing approximately 4×10^4 ferromagnetic Dy dots. We note that the sensitivity of the device is not restricted to such macroscopic sizes, a few periodically arranged dots are sufficient to observe similar effects. As for a 1D magnetic modulation, pronounced low field oscillations indicate the presence of a periodic magnetic field (effects associated with the quantum-mechanical Hofstadter energy spectrum[33] were not identified so far). The thin solid line in both figures are identical and obtained for a magnetization perpendicular to the 2DEG. The minimum position of this trace *between* the electric ($\lambda=2$) and magnetic ($\lambda=1$) flatband condition indicates that also an *electrostatic* periodic potential, again due to strain, contributes to the oscillatory resistance. A characteristic change of the oscillation pattern is observed if the magnetization vector is tilted from the z direction into the x [Fig. 6(a)] or the y direction [Fig. 6(b)]. This is done by applying the magnetizing field $B^{\max}$ in x or y direction, respectively, before the sample is rotated back into the measuring position with the magnetic field B_0 always oriented along the z axis. The higher the applied $B^{\max}$, the higher is the in-plane component of the magnetic stray field. While the oscillations in Fig. 6(a) *increase* with increasing $B^{\max}$, the oscillation amplitudes become *smaller* for increasing magnetizing fields in Fig. 6(b). The observed behavior is closely connected to the geometry of the stray field pattern

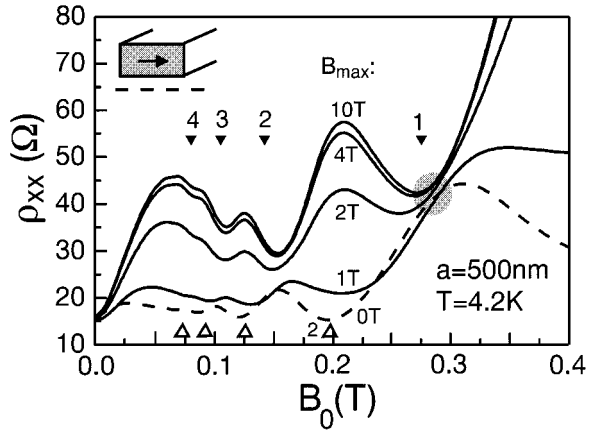

FIG. 5. Low-field ρ_{xx} traces for a Dy grating with $a=500$ nm measured at 4.2 K for $\mathbf{M}\|\hat{x}$ (see inset). The dashed trace, taken after initial cooldown, reflects pure *electrostatic* commensurability oscillations. Solid traces are taken after magnetizing the wires (from $B^{\max}=2$ T to 10 T) in the x direction. Contributions to ρ_{xx} resulting from increased magnetic modulation simply add to the electrostatically induced ρ_{xx} changes. This is clearly visible at the magnetic flatband condition $\lambda=1$ where the resistance minimum sits on the maximum of the dashed trace.

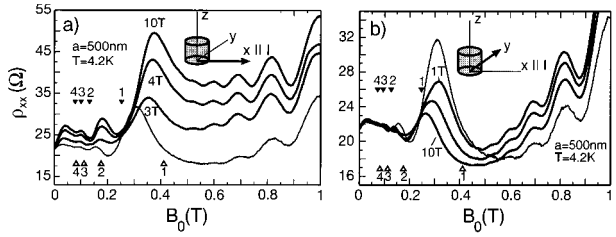

FIG. 6. ρ_{xx} vs B_0 for different directions of magnetization and magnetization strengths. The thin solid lines in both figures are obtained after magnetizing the dots in the z direction with $B^{\max}=10$ T. In (a) the magnetization is tilted towards the x direction by increasing $B^{\max}$, applied in x direction. The arrow in the inset illustrates the orientation of $B^{\max}$. Triangles mark the expected minima positions for pure magnetic (full symbols) and pure electrostatic modulation (open symbols), where the numbers are the corresponding λ values. (b) Like (a) but with $B^{\max}$ oriented along the y direction (see inset). With increasing $B_{\max}$ the magnetization component in the y direction increases. All measurements are carried out for B_0 oriented along the z direction.

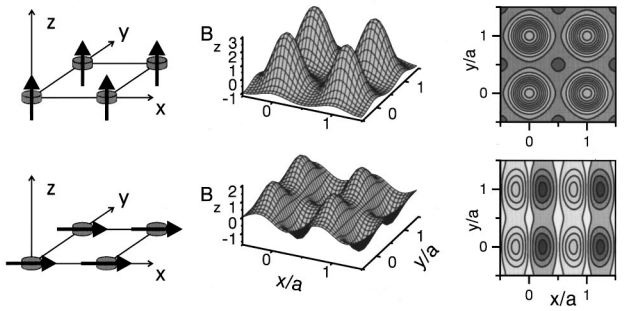

FIG. 7. Different orientations of the magnetization vector inside the magnetic dots (left hand side) and corresponding stray field pattern (z component) experienced by the electrons (middle row). The right row shows the corresponding contour plots illustrating the symmetry of the stray field pattern in the plane of the electron gas. The 2DEG is lying in the x-y plane.

relative to the orientation of the Hall bar. The effect of different orientations of **M** on the stray field pattern is illustrated in Fig. 7. If the magnetization is tilted towards the plane of the 2DEG, the square symmetric stray fields for magnetization $\mathbf{M}\|z$ (see Fig. 7, top row) become similar to the stray fields of ferromagnetic *wires* (Fig. 7, bottom row) with a magnetization parallel to the 2DEG.[24,34] Hence, the situation displayed in Fig. 6(a) is closely related to a situation where the current flows perpendicular to an array of in-plane magnetized ferromagnetic strips (1D modulation). A characteristic feature of this geometry is that the minima positions now nearly perfectly coincide with the positions expected for *pure* magnetic modulation. This is due to the phase change of the magnetic stray field pattern with respect to the strain induced electrostatic potential [similar to the situation sketched in Figs. 2(a) and 2(b)]. As discussed above, the Fourier coefficients $V_{\mathbf{q}}$ and $\omega_{\mathbf{q}}$ no longer have the same complex phase and the ''magnetic'' and ''electrostatic'' contributions to the resistivity are simply added up.[21,24,34] Hence, the minima positions are close to the expected magnetic field values for the magnetic flatband condition and the presence of the electrostatic periodic potential is manifested by an increased (oscillatory) resistance level. In Fig. 6(b), on the other hand, the current flow is parallel to the 1D-like magnetic field modulation. For a strict 1D modulation of the magnetic field, the oscillations due to the magnetic modulation may be completely suppressed as the alternating magnetic fields ''guide'' the electrons with increasing $B^{\max}$ in the direction of the current flow. Hence, the ''magnetic'' contribution to σ_{yy} (and therefore to ρ_{xx}) becomes smaller with increasing $B^{\max}$ and the remaining oscillatory features become successively dominated by the electrostatic periodic potential. This picture is consistent with the observation that the oscillation amplitude in Fig. 6(b) decreases with growing $B^{\max}$ and that the oscillation minima shift closer to the ''electric'' flatband conditions.

ACKNOWLEDGMENTS

The work was carried out in close collaboration with K. von Klitzing, G. Lütjering, M. Seeger, K. Eberl, and H. Nickel. We like to thank M. Riek, U. Waizmann, and B. Schönherr for technical assistance. The work was supported by the German Bundesministerium für Bildung und Forschung (BMBF).

[1] *Nanomagnetism*, edited by A. Hernando (Kluwer Academic, Dordrecht, 1993), and references therein.
[2] J. F. Smyth, S. Schultz, D. R. Fredkin, D. P. Kern, S. A. Rishton, H. Schmid, M. Cali, and T. R. Koehler, J. Appl. Phys. **69**, 5262 (1991).
[3] D. D. Awschalom, M. A. McCord, and G. Grinstein, Phys. Rev. D **65**, 783 (1990).
[4] B. Voightlander, G. Mayer, and N. M. Amer, Phys. Rev. B **44**, 10354 (1991).
[5] D. D. Awschalom, J. R. Rozen, M. B. Ketchen, W. J. Gallagher, A. W. Kleinsasser, R. L. Sandstrom, and B. Bumble, Appl. Phys. Lett. **53**, 2108 (1988).
[6] A. M. Chang, H. D. Hallen, L. Harriott, H. F. Hess, H. L. Kao, J. Kwo, R. E. Miller, R. Wolfe, J. van der Ziel, and T. Y. Chang, Appl. Phys. Lett. **61**, 1974 (1992).
[7] A. D. Kent, S. von Molńar, S. Gider, and D. D. Awschalom, J. Appl. Phys. **76**, 6656 (1994).
[8] P. Grutter, H. J. Mamin, and D. Rugar, in *Scanning Tunneling Microscopy II*, edited by R. Wiesendanger and H.-J. Güntherodt (Springer, Berlin, 1992).
[9] M. Hehn, K. Ounadjela, J.-P. Bucher, F. Rosseaux, D. Decanini, B. Bartenlian, and C. Chappert, Science **272**, 1782 (1996).
[10] M. Löhndorf, A. Wadas, G. Lütjering, D. Weiss, and R. Wiesendanger, Z. Phys. B **101**, 1 (1996).
[11] J. G. Th. te Lintelo, J. C. Lodder, S. McVitie, and J. N. Chapman, J. Appl. Phys. **75**, 3002 (1994).
[12] C. W. J. Beenakker and H. van Houten, in *Solid State Physics*, edited by H. Ehrenreich and D. Turnbull (Academic, New York, 1991), Vol. 44.
[13] K. von Klitzing, G. Dorda, and M. Pepper, Phys. Rev. Lett. **45**, 494 (1980).
[14] T. Chakraborty and P. Pietiläinen, *The Quantum Hall Effects, Solid State Sciences* (Springer, Berlin, 1995), Vol. 85.
[15] H. van Houten, B. J. van Wees, J. E. Mooij, C. W. J. Beenakker, J. G. Williamson, and C. T. Foxon, Europhys. Lett. **5**, 721 (1988).
[16] B. J. van Wees, H. van Houten, C. W. J. Beenakker, J. G. Williamson, L. P. Kouwenhoven, D. Van der Marel, and C. T. Foxon, Phys. Rev. Lett. **60**, 848 (1988).
[17] D. A. Wharam, T. J. Thornton, R. Newbury, M. Pepper, H. Ahmed, J. E. F. Frost, D. G. Hasko, D. C. Peacock, D. A. Ritchie, and G. A. C. Jones, J. Phys. C **21**, L209 (1988).
[18] D. Weiss, K. von Klitzing, K. Ploog, and G. Weimann, Europhys. Lett. **8**, 179 (1989).
[19] D. Weiss, M. L. Roukes, A. Menschig, P. Grambow, K. von Klitzing, and G. Weimann, Phys. Rev. Lett. **66**, 2790 (1991).
[20] P. Vasilopoulos and F. M. Peeters, Superlattices Microstruct. **7**, 393 (1990).
[21] F. M. Peeters and P. Vasilopoulos, Phys. Rev. B **47**, 1466 (1993).
[22] D. P. Xue and G. Xiao, Phys. Rev. B **45**, 5986 (1992).
[23] R. Yagi and Y. Iye, J. Phys. Soc. Jpn. **62**, 1279 (1993).
[24] R. R. Gerhardts, Phys. Rev. B **53**, 11 064 (1996).
[25] H. A. Carmona, A. K. Geim, A. Nogaret, P. C. Main, T. J. Foster, M. Henini, S. P. Beaumont, and M. G. Blamire, Phys. Rev. Lett. **74**, 3009 (1995).
[26] P. D. Ye, D. Weiss, R. R. Gerhardts, M. Seeger, K. von Klitzing, K. Eberl, and H. Nickel, Phys. Rev. Lett. **74**, 3013 (1995).
[27] S. Izawa, S. Katsumoto, A. Endo, and Y. Iye, J. Phys. Soc. Jpn. **64**, 706 (1995).
[28] R. R. Gerhardts, D. Weiss, and K. von Klitzing, Phys. Rev. Lett. **62**, 1173 (1989).
[29] R. W. Winkler, J. P. Kotthaus, and K. Ploog, Phys. Rev. Lett. **62**, 1177 (1989).
[30] C. W. J. Beenakker, Phys. Rev. Lett. **62**, 2020 (1989).
[31] P. D. Ye, D. Weiss, R. R. Gerhardts, K. von Klitzing, K. Eberl, H. Nickel, and C. T. Foxon, Semicond. Sci. Technol. **10**, 715 (1995).
[32] J. H. Davies and I. A. Larkin, Phys. Rev. B **49**, 4800 (1994).
[33] R. R. Gerhardts, D. Pfannkuche, and V. Gudmundsson, Phys. Rev. B **53**, 9591 (1996).
[34] P. D. Ye, D. Weiss, R. R. Gerhardts, G. Lütjering, K. von Klitzing, and H. Nickel, Semicond. Sci. Technol. **11**, 1613 (1996).